Comprehensive Surfaceome Profiling to Identify and Validate Novel Cell-Surface Targets in Osteosarcoma

Yifei Wang[1], Xiangjun Tian[2], Wendong Zhang[1], Zhongting Zhang[1], Rossana Lazcano[3], Pooja Hingorani[1], Michael E. Roth[1], Jonathan D. Gill[1], Douglas J. Harrison[1], Zhaohui Xu[1], Sylvester Jusu[1], Sankaranarayanan Kannan[1], Jing Wang[2], Alexander J. Lazar[3], Eric J. Earley[4], Stephen W. Erickson[4], Tara Gelb[5], Philip Huxley[6], Johanna Lahdenranta[5], Gemma Mudd[6], Raushan T. Kurmasheva[7], Peter J. Houghton[7], Malcolm A. Smith[8], Edward A. Kolb[9], and Richard Gorlick[1]

ABSTRACT

Immunoconjugates targeting cell-surface antigens have demonstrated clinical activity to enable regulatory approval in several solid and hematologic malignancies. We hypothesize that a rigorous and comprehensive surfaceome profiling approach to identify osteosarcoma-specific cell-surface antigens can similarly enable development of effective therapeutics in this disease. Herein, we describe an integrated proteomic and transcriptomic surfaceome profiling approach to identify cell-surface proteins that are highly expressed in osteosarcoma but minimally expressed on normal tissues. Using this approach, we identified targets that are highly expressed in osteosarcoma. Three targets, MT1-MMP, CD276, and MRC2, were validated as overexpressed in osteosarcoma. Furthermore, we tested BT1769, an MT1-MMP–targeted *Bicycle* toxin conjugate, in osteosarcoma patient-derived xenograft models. The results showed that BT1769 had encouraging antitumor activity, high affinity for its target, and a favorable pharmacokinetic profile. This confirms the hypothesis that our approach identifies novel targets with significant therapeutic potential in osteosarcoma.

Introduction

Osteosarcoma is the most common primary malignant bone tumor in adolescents and young adults. The survival rate for patients with localized disease is 60% to 70% (1); metastatic disease leads to a poor survival rate of 20% to 30% (2). The outcome of patients with osteosarcoma has not improved in the last several decades since the implementation of adjuvant chemotherapy. Although tremendous advances in recent studies using whole-genome sequencing have shown the high complexity of the osteosarcoma genome, few recurrent targetable alterations have been identified (3). Moreover, pediatric solid tumors tend to have low mutational burden, and checkpoint

[1]Department of Pediatrics, Children's Cancer Hospital, The University of Texas MD Anderson Cancer Center, Houston, Texas. [2]Department of Bioinformatics and Computational Biology, The University of Texas MD Anderson Cancer Center, Houston, Texas. [3]Departments of Pathology & Genomic Medicine, The University of Texas MD Anderson Cancer Center, Houston, Texas. [4]RTI International, Research Triangle Park, North Carolina. [5]Bicycle Therapeutics, Lexington, Massachusetts. [6]Bicycle Therapeutics, Babraham Research Campus, Cambridge, United Kingdom. [7]Greehey Children's Cancer Research Institute, The University of Texas Health Science Center at San Antonio, San Antonio, Texas. [8]Cancer Therapy Evaluation Program, NCI, Bethesda, Maryland. [9]Division of Pediatric Hematology/Oncology, A.I. duPont Hospital for Children, Wilmington, Delaware.

inhibitors have not shown sufficient antitumor activity (4). Thus, new treatment strategies are urgently needed.

Immunotherapies targeting cell-surface antigens, such as therapeutic monoclonal antibodies (mAb), chimeric antigen receptor (CAR) T cells, and immunoconjugates such as antibody-drug conjugates (ADC), have shown promising efficacy in hematologic malignancies and solid tumors (5–7). Several mAbs and ADCs have been tested in clinical trials for osteosarcoma (8–12). Although HER2, IGF1R, GD2, and GPNMB were found to be expressed in some osteosarcoma samples (13–15), mAbs or ADCs for these targets failed to show sufficient antitumor activity in clinical trials (8, 9, 11, 12). One potential reason might be the low expression level of the surface antigens. Ideally, cell-surface antigens to be used as immunotherapeutic targets should have high expression level on the tumor while limited expression on normal tissues (13–16). However, the surfaceome of osteosarcoma has not yet been fully studied. The lack of known tumor-specific cell-surface antigens has been a major obstacle for the development of future therapy for osteosarcomas.

In the current study, we sought to identify targetable cell-surface antigens with therapeutic potential in osteosarcoma. We employed a high-throughput integrated approach using proteomic and transcriptomic data from osteosarcoma cell lines, patient-derived xenograft (PDX) tissue, and patient samples to identify high-confidence osteosarcoma cell-surface antigens. Our data demonstrated that MT1-MMP (MMP14), MRC2 (uPARAP/endo180), and CD276 (B7-H3) were highly expressed in osteosarcoma.

MT1-MMP is currently being explored as a therapeutic target in a Phase I/II clinical trial (NCT03486730) with the *Bicycle* toxin conjugate (BTC), BT1718. BTCs consist of constrained bicyclic peptides that have low nanomolar affinity to their target and, like ADCs, are designed to release a cytotoxic payload in the tumor microenvironment (17). In contrast to ADCs, BTCs have a low molecular weight (∼4.5 kDa), which enables rapid tumor penetration and a shorter systemic half-life to help minimize toxicity (18). However, MT1-MMP targeted therapy has not been tested in osteosarcomas before.

As a proof of principle that we had identified osteosarcoma relevant targets for toxin delivery, we tested a second-generation MT1-MMP–targeted BTC, BT1769, against osteosarcoma PDX models under the auspices of the NCI's Pediatric Preclinical Testing Consortium (PPTC). BT1769 significantly inhibited tumor growth in all osteosarcoma PDX models tested, further supporting clinical development of MT1-MMP–targeted therapies in osteosarcoma.

Materials and Methods

PDX models

PDX models were available through the PPTC, an NCI-funded program to evaluate novel agents against pediatric solid tumor and leukemia preclinical models. All these models have been characterized through multiple approaches (19, 20), and all the current available data on these models can be found at PedcBioPortal (https://pedcbioportal. kidsfirstdrc.org/study/summary?id=pptc). We used 10 osteosarcoma PDX models (OS1, OS9, OS29, OS31, OS33, OS34, OS36, OS42, OS55, and OS60) for proteomic analysis and an additional 9 models (OS2, OS17, OS21, OS39, OS43, OS46, OS51, OS56, and OS58) for IHC analysis. Six osteosarcoma PDX models and 2 Ewing sarcoma models were used for *in vivo* testing.

Cell culture

The following standard osteosarcoma cell lines were purchased from ATCC: 143B (ATCC CRL-8303), U2OS (ATCC HTB-96), HOS (ATCC CRL-1543), Saos-2 (ATCC HTB-85), and MG-63 (ATCC CRL-1427). We used 4 patient-derived osteosarcoma cell lines (OS301, OS355, OS322, and OS343) for proteomic analysis, 3 cell lines (OS252, OS255, and OS373) for Western blotting and flow cytometry analysis, and an additional 13 cell lines (OS242, OS300, OS308, OS337, OS340, OS342, OS354, OS365, OS366, OS368, OS377, OS379, and OS396) for RNA sequencing (RNA-seq) analysis. Five xenograft cell lines (OS17, OS31, OS33, OS39, and OS43) were used for flow cytometry analysis. All patient-derived osteosarcoma cell lines and xenograft cell lines were established as described previously (19, 21). These cell lines were cultured in DMEM (#30–2002, ATCC) with 10% FBS (# Mt35011cv, Fisher Scientific) in a humidified incubator at 37°C with 5% CO_2. All cell lines were negative for Mycoplasma contamination (MycoAlert, Lonza LT07–118).

Computational identification of candidate immunotherapeutic targets in osteosarcoma

RNA-seq data from the 101 TARGET osteosarcoma tumors and 29 GTEx normal tissues ($n = 16,695$) were retrieved. Differential expression was tested by the R package DESeq2 (v1.28.1) to obtain log fold changes (LFC) and q values (or FDR-adjusted P values). Only genes that were overexpressed in osteosarcoma in contrast to all 29 normal tissues (LFC > 1, q < 0.01) were considered as potential candidates.

For osteosarcoma and normal tissue protein-level differential expression analysis, a set of normalized intensity-based proteomic data of osteosarcoma and 24 normal tissues ($n = 70$) was retrieved by the application programming interface of ProteomicsDB (www.proteomicsdb.org/#api, 12–12–2019, RRID:SCR_015562). We tested the differential expression by calculating the fold change.

We further analyzed mass spectrometry data we obtained from the osteosarcoma cell lines ($n = 8$) and PDX models ($n = 10$). Only proteins overexpressed in osteosarcoma tumor compared with normal tissue (minimum fold change >1) and highly expressed in cell lines and PDX models were selected.

Finally, surface proteins that were enriched at both mRNA and protein levels were selected as candidates for further investigation.

Membrane protein extraction and mass spectrometry identification

Plasma membrane protein extraction from osteosarcoma cell lines and PDX models was done using a Mem-PER Plus Membrane Protein Extraction Kit (Thermo Scientific, 89842) according to the manufacturer's instructions. Biological replicates of all the cell lines and PDXs were prepared.

Cell lysates were precipitated with 5 volumes of cold acetone at –20°C overnight. Precipitates were resuspended and digested with 500-ng modified trypsin (sequencing grade, Promega) and RapiGest surfactant (Waters Corp.) in 50-mmol/L tetraethylammonium bicarbonate for 18 hours at 37°C. The resulting peptides were extracted and analyzed by high-sensitivity liquid chromatography with tandem mass spectrometry on an Orbitrap Fusion Mass Spectrometer (Thermo Scientific).

Proteins were identified by searching for the fragment spectra in the SwissProt (European Bioinformatics Institute) protein database using Mascot (v 2.6, Matrix Science) or Sequest HT and Proteome Discoverer (v 2.2, Thermo Scientific, RRID:SCR_014477). Typical search settings were mass tolerances, 10-ppm precursor, 0.8d fragments; variable modifications, methionine sulfoxide, pyro-glutamate formation; enzyme, trypsin, up to 2 missed cleavages. Peptides were subject to 1% FDR using reverse-database searching. The abundance of a protein was measured by a spectral count–based method yielding total number of peptide spectrum matches, which was further normalized to derive the normalized spectral abundance factor (22).

Tumor and normal tissue RNA expression profiling

The gene expression profiling of 17 osteosarcoma cell lines was obtained by 150-bp paired-end RNA-seq with an average coverage of 26.5 (23.3–29.4) million reads. The quality of the reads was checked by FastQC (v 0.11.8, RRID:SCR_014583), and then the reads were mapped against human genome GRCh38.p12 by TopHat2 (v 2.1.1). The mapped reads were counted for each gene by HTSeq (v 0.11.0, RRID:SCR_005514) based on the annotation of GENCODE v 29 (GRCh38.p12, RRID:SCR_014966).

The RNA-seq expression data of 101 samples of patients with osteosarcoma were downloaded from the TARGET data matrix (https://ocg.cancer.gov/programs/target/data-matrix, 05–29–2019), among which 98 samples came with detailed clinical data. Another set of RNA-seq expression data including 2007 samples of 16 types of pediatric cancers was retrieved from the St. Jude PeCan Data Portal (https://pecan.stjude.cloud/proteinpaint, 04–07–2020).

The normal tissue RNA-seq expression data were downloaded from the Genotype-Tissue Expression Project (GTEx V8, 08–26–2019; https://www.gtexportal.org), which includes 29 types of normal tissue including 16,695 samples.

Cell-surface protein prediction

To identify the proteins localized to the plasma membrane, a pool of 6,647 plasma membrane proteins were retrieved from the subcellular localization database Compartments (https://compartments.jensen lab.org/; ref. 23), the subcellular location data of the Human Protein Atlas (HPA) v19 (www.proteinatlas.org), and the Membranome 2.0 database (24). The pool was composed of Compartments proteins that are localized on the plasma membrane (GO:0005622) with confidence score > 3.0 ($n = 5,877$), HPA proteins that are annotated with the plasma membrane as the main location or additional location

(n = 1,575), and Membranome 2.0 proteins defined by membrane_name_cache = "Plasma memb.", membrane_id = "1", and species_name_cache = "Homo sapiens" (n = 1,347).

Overall survival analysis

We applied the Kaplan–Meier estimator method to perform overall survival analyses for the TARGET data set patients with osteosarcoma with available survival endpoints (n = 95) using the R packages survival (v3.2–7) and survminer (v0.4.8). The TARGET cohort was segregated into 2 groups based on gene expression, with a cutoff between the highest 50% (high) and the lowest 50% (low).

Western blotting

Cell extracts were prepared with RIPA buffer (Cell Signaling Technology, 9806) as a protein extraction reagent plus a protease/phosphatase inhibitor cocktail (Cell Signaling Technology, 5872). The cell lysates were separated on a 10% SDS-PAGE and transferred with a Trans-Blot Turbo RTA Mini 0.2 µm Nitrocellulose Transfer Kit (Bio-Rad, 1704270). The membranes were blocked with blocking buffer (VWR international, AAJ60473AP) at room temperature for 2 hours, then incubated with primary antibody at 4°C overnight. The following primary antibodies were used: MT1-MMP (Abcam, ab51074, 1:5,000), MRC2 (Abcam, ab71032, 1:1,000), CD276 (Abcam, ab219648, 1:1,000), Cofilin (Abcam, ab124979, 1:1,000), and β-actin (Cell Signaling Technology, 4967, 1:1,500). The membranes were then incubated with horseradish peroxidase–conjugated goat anti-rabbit secondary antibody (Cell Signaling Technology Catalog No. 7074, RRID:AB_2099233, 1:1,000) at room temperature for 1 hour. Western blotting was performed with Clarity Western ECL substrate (Bio-Rad, #170–5060). The ChemiDoc System (Bio-Rad) was used for images.

IHC analysis and H-scores

IHC staining was performed on formalin-fixed, paraffin-embedded tissue microarrays of samples of 37 patients with osteosarcoma (25, 26), 19 PDX models, and 14 normal human tissue samples. Sections were stained with mouse or rabbit anti-human mAbs against MT1-MMP (Abcam, ab51074, 1:400), MRC2 (Abcam, ab70132, 1:200), and CD276 (Abcam, ab219648, 1:100). All sections were counterstained with hematoxylin, dehydrated, and mounted. Sections were processed with peroxidase-conjugated avidin/biotin and 3,3′-diaminobenzidine substrate (Leica Microsystems). Slides were scanned and digitalized using a ScanScope XT system (Aperio/Leica Technologies). The quantitative analysis of the IHC staining was performed by a pathologist (R. Lazcano) using microscope direct observation. The results were expressed as membrane and cytoplasmic positivity in tumor cells, PDX, and normal tissue in the form of the H-score (intensity × % cells; 0 to 300). Cytoplasm staining was also observed. Representative images were obtained from scanned IHC slides with Halo software v3.1.1 (Indica Labs, RRID:SCR_018350).

Flow cytometry analyses

The osteosarcoma cell lines were analyzed for MT1-MMP, MRC2, and CD276. Samples with 10^6 cells were washed twice with PBS and resuspended in PBS-1% BSA. Antibodies for MT1-MMP (R&D Systems, FAB9181A, 1:40), MRC2 (kindly provided by Dr. Niels Behrendt, University of Copenhagen, Copenhagen, Denmark, clone 2h9, 1:500; ref. 27), and CD276 (R&D Systems, FAB1027P, 1:40) were added. After incubation for 30 minutes on ice in the dark, the cells were washed twice with PBS-1% BSA. Flow cytometry was performed using a FACS Fortessa instrument (BD Biosciences) and analyzed with FlowJo software (FlowJo, LLC, RRID:SCR_008520). Respective unstained control cells were used to set voltages for forward scatter, side scatter, and fluorescence.

Synthesis of BT1769

BT1769 was prepared as previously described (compound referred to as BT17BDC61; ref. 28).

Surface plasmon resonance analysis of BT1769

Biacore experiments were performed to determine k_a [(mol/L)$^{-1}$s^{-1}], k_d (s^{-1}), and K_D (nmol/L) values of BT1769 binding to human and mouse MT1-MMP.

Preparation of the recombinant human MT1-MMP and mouse MT1-MMP hemopexin domain was carried out as previously described (29). Proteins were biotinylated in acidic buffer for 1 hour using EZ-Link Sulfo-NHS-LC-Biotin (Thermo Fisher) with a 4x excess. Non-reacted biotin was removed by dialysis.

For analysis of MT1-MMP peptide binding, a Biacore 3000 instrument with a Biacore CM5 chip (GE Healthcare) was used. Streptavidin was immobilized on the chip using standard amine-coupling chemistry at 25°C with HBS-N (10-mmol/L HEPES, 0.15 mol/L NaCl, pH 7.4) as the running buffer. Briefly, the carboxymethyl dextran surface was activated with a 7-minute injection of a 1:1 ratio of 0.4 mol/L 1-ethyl-3-(3-dimethylaminopropyl) carbodiimide hydrochloride/0.1 mol/L N-hydroxy succinimide at a flow rate of 10 µL/min. For the capture of streptavidin, the protein was diluted to 0.2 mg/mL in 10-mmol/L sodium acetate (pH 4.5) and captured by injecting 120 µL into the activated chip surface. Residual activated groups were blocked with a 7-minute injection of 1 mol/L ethanolamine (pH 8.5):HBS-N (1:1). Biotinylated human and rat/mouse MT1 MMP were captured to a level of 1,200 and 1,100 RU respectively using a dilution of protein to 0.5 µmol/L (human protein) and 0.2 µmol/L (rat/mouse protein) in HBS-N buffer at a flow rate of 3 µL/min. The buffer was then changed to running buffer (10 mmol/L HEPES, pH 7.4, 150 mmol/L NaCl, 1 mmol/L CaCl$_2$, 0.025% Tween 20, and 1% DMSO). A dilution series of the peptides was prepared in this buffer with a final DMSO concentration of 1% with a top peptide concentration of 100 nmol/L and 6 further 2-fold dilutions. The SPR analysis was run at 25°C at a flow rate of 50 µL/min with 60 seconds association and 400 seconds dissociation.

Data were corrected for DMSO excluded volume effects. All data were double referenced for blank injections and reference surface using standard processing procedures, and data processing and kinetic fitting were performed using Scrubber software, version 2.0c (BioLogic Software, RRID:SCR_015745). Data were fitted using a simple 1:1 binding model allowing for mass transport effects.

HT1080 tumor xenograft studies

Female BALB/c nude mice (Shanghai Lingchang Biotechnology Experimental Animal Co., Ltd.), age 6 to 8 weeks, were inoculated subcutaneously with $10 \times 10 + e6$ HT1080 tumor cells. Animals were randomized for the vehicle (25 mmol/L histidine, 10% sucrose, pH 7) and BT1769 treatment groups when average tumor volume reached 195 mm^3 (efficacy study) or 430 mm^3 (pharmacokinetic study). Mice were treated with a single dose (pharmacokinetic study) or weekly doses of the vehicle or 3.2 mg/kg BT1769 intravenously. Tumor growth was monitored with caliper measurements. For the plasma and tumor pharmacokinetic analysis, mice were euthanized for tissue collection, and BT1769 and monomethyl auristatin E (MMAE) levels were quantified in plasma and tumor samples following analyte extraction and bioanalysis using liquid chromatography with tandem mass spectrometry on a Hybrid Triple Quadrupole/Linear Ion trap mass
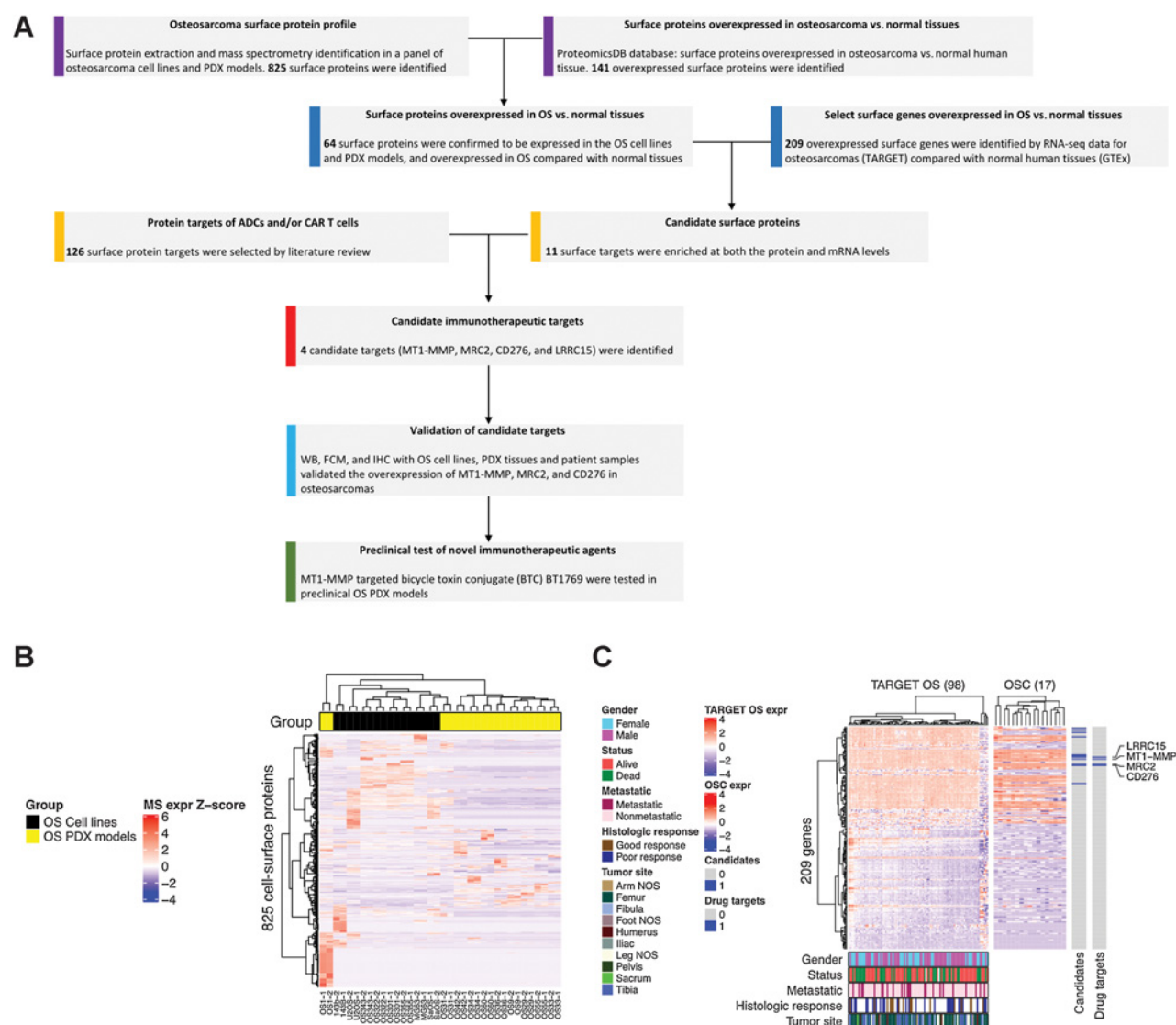
Figure 1.
Integrative proteomic and transcriptomic surfaceome profiling of osteosarcoma. **A,** The workflow of the integrative proteomic and transcriptomic approach used to identify immunotherapeutic targets in osteosarcomas. **B,** Expression profile of the cell-surface proteins identified by mass spectrometry in osteosarcoma cell lines and PDX models. **C,** Expression profile of the 209 overexpressed surface protein-encoding genes in 98 patients with osteosarcoma from the TARGET database (TARGET OS) and 17 osteosarcoma cell lines that we analyzed (OSC). The 11 candidate surface proteins and the 4 candidates that overlapped with existing drug targets are marked. The 4-candidate targets (MT1-MMP, MRC2, CD276, and LRRC15) were highly expressed in most of the patient samples and cell lines.

spectrometer. HT1080 xenograft and BT1769 pharmacokinetic studies were conducted at Wuxi AppTec Co. Ltd. (Beijing, China). All the procedures related to animal handling, care, and treatment in the studies were performed in accordance with and with the approval of the Institutional Animal Care and Use Committee (IACUC) of WuXi AppTec, following the guidance of the Association for Assessment and Accreditation of Laboratory Animal Care.

Preclinical trials

CB17SC scid$^{-/-}$ female mice (5–8 weeks) were used to propagate subcutaneous flank xenografts from 6 osteosarcoma and 2 Ewing sarcoma PDX models. All mice handling and treatment were conducted in accordance with and with the approval of the IACUC at MD Anderson. Ten mice were used in each control or treatment group. BT1769 was administered via intravenous injection at a dose of 3 mg/kg in vehicle (25 mmol/L Histidine, 10% sucrose pH 7) once per week for 4 consecutive weeks in all 8 models. A control cohort that received 100 µL/10 g vehicle was included for all PDX models assessed. Treatment was initiated when tumor volumes reached 200 mm^3, and tumor volume and survival were monitored biweekly as previously described (19).

The *in vivo* activity of BT1769 was evaluated using standard PPTC methods. Briefly, an event was defined as a quadrupling of tumor volume from day 0. The median time to event was assessed between the experimental and control cohorts. Differences in event-free survival (EFS) between experimental groups were tested with α = 0.05, 2-sided
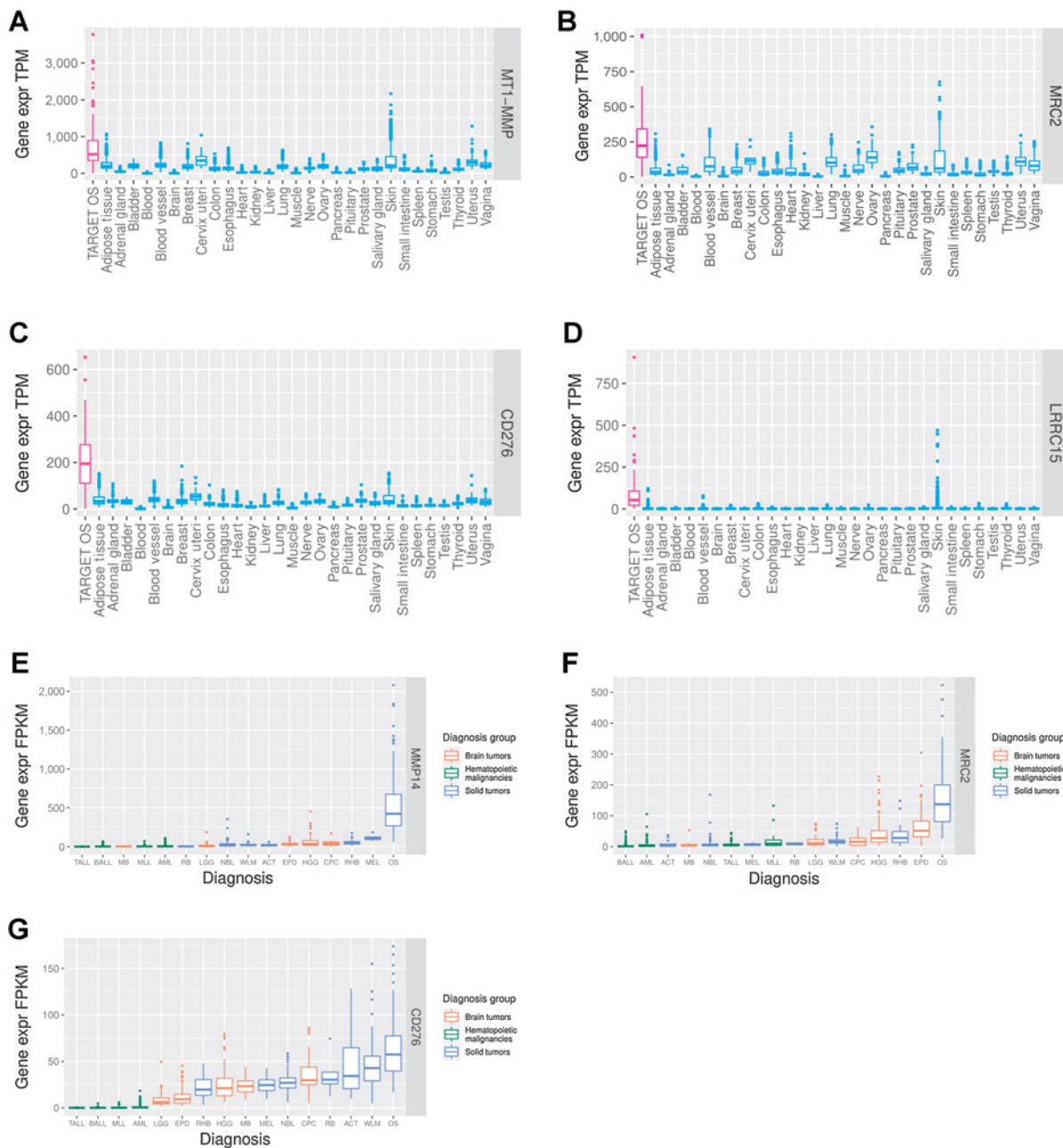
Figure 2.
mRNA expression of MT1-MMP, MRC2, CD276, and LRRC15 in osteosarcoma, normal tissues, and other pediatric cancers. **A–D,** RNA-seq data showed MT1-MMP (**A**), MRC2 (**B**), CD276 (**C**), and LRRC15 (**D**) were overexpressed in osteosarcoma compared with a range of normal tissues. The boxes represent the Q1 and Q3 of the data. The bars represent the median. **E–G,** MT1-MMP (**E**), MRC2 (**F**), and CD276 (**G**) had higher expression in osteosarcoma compared with other pediatric cancers (OS, osteosarcoma; MEL, melanoma; RHB, rhabdomyosarcoma; CPC, choroid plexus carcinoma; HGG, high-grade glioma; EPD, ependymoma; ACT, adrenocortical carcinoma; WLM, Wilms' tumor; NBL, neuroblastoma; LGG, low-grade glioma; RB, retinoblastoma; AML, acute myeloid leukemia; MLL, mixed-lineage leukemia; MB, medulloblastoma; BALL, B-cell acute lymphoblastic leukemia; TALL, T-cell acute lymphoblastic leukemia). FPKM, fragments per kilobase million; TPM, transcripts per million.

alternative with ρ = 1, which is equivalent to the Peto and Peto modification of the Gehan–Wilcoxon test. Objective responses were reported for each model as maintained complete response (MCR), complete response, partial response, and stable disease, as defined previously (19). Further details of the statistical analysis are provided in the Supplementary Methods.

Results

Proteomic analysis identifies overexpressed cell-surface proteins in osteosarcoma

Figure 1A summarizes our stepwise approach to identifying therapeutic targets in osteosarcoma. Quantitative mass spectrometry identified 2,683 proteins from surface protein extracts, 825 of which

were annotated as plasma membrane proteins. Unsupervised hierarchical clustering was used to show the expression profile of the cell-surface proteins (**Fig. 1B**).

Also, we obtained the proteomics data for osteosarcoma tissue and normal human tissues (Supplementary Table S1) from the public database ProteomicsDB (30) and identified 141 proteins as overexpressed in osteosarcoma (fold change >1). Then we integrated these two proteomic datasets; 64 surface proteins were confirmed to be both expressed in the osteosarcoma cell lines and PDX models and overexpressed in osteosarcoma compared with normal tissues (**Fig. 1A**).

Integrative transcriptomic and proteomic analysis identifies MT1-MMP, MRC2, and CD276 as high-confidence overexpressed cell-surface proteins in osteosarcoma

We first compared RNA-seq data from patients with osteosarcoma and normal tissues. We identified 604 genes were highly expressed in osteosarcomas (log2 fold change > 1, q < 0.01). Among the 604 genes, 209 genes encoding plasma membrane proteins were predicted. Next, hierarchical clustering analysis was used to illustrate the expression patterns of the 209 candidate surface protein-encoding genes in the patients with osteosarcoma from the TARGET data set and in 17 osteosarcoma cell lines (**Fig. 1C**).

We then integrated the proteomic and transcriptomic data and found 11 candidate surface proteins that were overexpressed at both

the mRNA and protein levels in osteosarcoma compared with normal tissues (**Fig. 1A**). We then cross-referenced the targets of ADCs and CAR-T cells and other cell-surface targeted agents (Supplementary Table S2) with the 11 candidate surface proteins. We identified 4 proteins—MT1-MMP, MRC2, CD276, and LRRC15—that were overexpressed in osteosarcoma (**Fig. 2A–D**) and have been used as drug targets (**Fig. 1A**).

Previously, we have reported the expression of LRRC15 in osteosarcomas and a preclinical test of an LRRC15-targeted ADC (ABBV-085; ref. 31). Therefore, in the current study we prioritized MT1-MMP, MRC2, and CD276 for further validation. Survival analysis show the expression levels of the 3 targets did not affect survival (Supplementary Fig. S1A–C). Also, the expression levels of MT1-MMP, MRC2, and CD276 in osteosarcoma were higher compared with 15 other types of pediatric cancers (**Fig. 2E–G**) based on RNA-seq data from 2007 patient samples in the St. Jude PeCan Data Portal.

Validation of MT1-MMP, MRC2, and CD276 as cell-surface antigens in osteosarcoma

Western blotting was used to confirm the expression of MT1-MMP, MRC2, and CD276 in 8 osteosarcoma cell lines and 8 PDX models (**Fig. 3A, B**). Flow cytometry was performed to validate the cell-surface localization and the expression levels of the 3 candidate targets in 7 osteosarcoma cell lines (**Fig. 3C**).
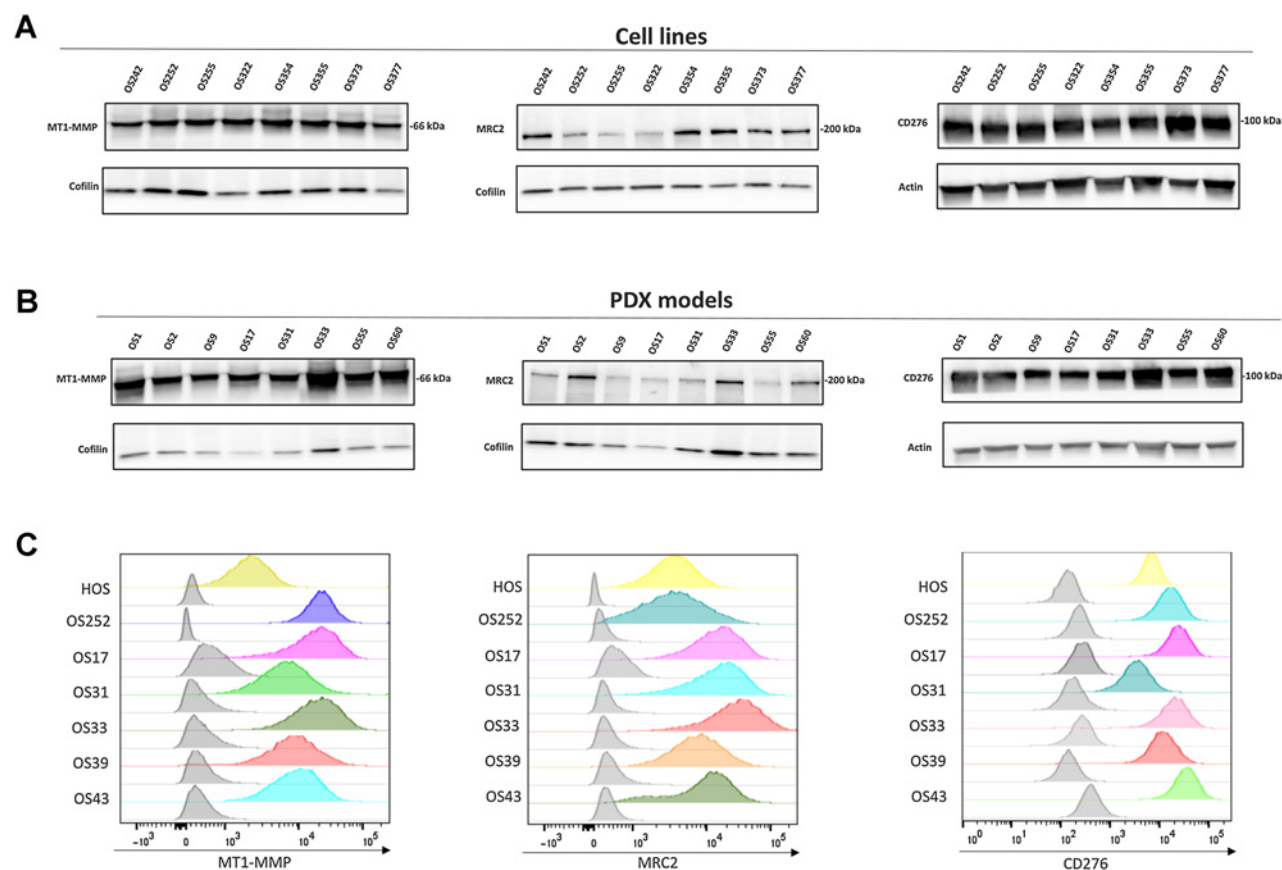
Figure 3.
MT1-MMP, MRC2, and CD276 are highly expressed cell-surface proteins in osteosarcoma. **A** and **B,** Western blots of MT1-MMP, MRC2, and CD276 in a panel of osteosarcoma cell lines ($n = 8$; **A**) and PDXs ($n = 8$; **B**). **C,** Flow cytometry analysis of 7 osteosarcoma cell lines. Gray plots represent unstained controls, and colored plots represent staining with MT1-MMP, MRC2, and CD276 antibodies.
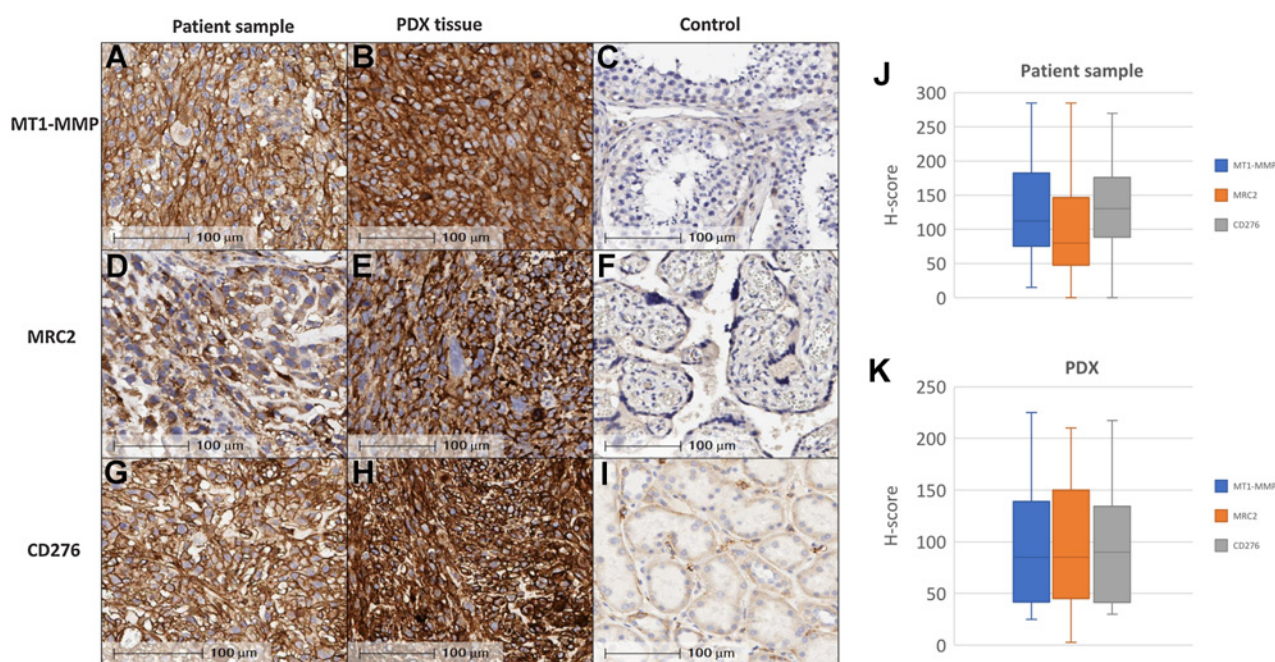
Figure 4.
IHC staining showed high membranous positivity of MT1-MMP, MRC2, and CD276 in most osteosarcoma patient samples and PDXs. **A–C,** Representative membrane-staining examples of MT1-MMP in a patient sample (**A**), PDX (**B**), and testes (negative control; **C**). **D–F,** Representative membrane-staining examples of MRC2 in a patient sample (**D**), PDX (**E**), and placenta (negative control; **F**). **G–I,** Representative membrane-staining examples of CD276 in a patient sample (**G**), PDX (**H**), and placenta (mild positive; **I**). **J** and **K,** Summary of IHC staining H-score of MT1-MMP, MRC2, and CD276 in the tissue microarray for 37 patients with osteosarcoma (**J**) and 19 PDX models (**K**). Boxes indicate SD, and error bars represent data range.

We then performed IHC staining using an osteosarcoma tissue microarray from 37 patients and 19 PDX models; results are shown in **Fig. 4A–K**. MT1-MMP was found to be expressed in all the patient samples and 97% of the PDXs. MRC2 was expressed in 97% of the patient samples and 95% of the PDXs. CD276 was expressed in all the patient samples and the PDXs.

MT1-MMP, MRC2, and CD276 are not highly expressed in most normal tissues

We also performed IHC staining on 13 normal tissues on the microarray (Supplementary Fig. S2). We observed high (3+) MT1-MMP intensity in gastric glands; moderate (2+) intensity in placenta villous cells, tonsil, small intestine glands, and pancreatic cells; and low (1+) intensity in colonic glands, renal tubules, and skin dermis and adnexa. MT1-MMP was negative in ovary stroma, testes, hepatocytes, skeletal muscle, and cardiac muscle.

MRC2 was expressed in few normal tissues. The gastric mucosa specifically on the base of the glands had high-intensity (3+) staining. The rest of the organs that had mild (1+) expression; these were the ovary stroma, Leydig cells of the testes, hepatocytes, colon gland cells, and cardiac muscle cells. The placenta, tonsil, kidney, small intestine, skeletal muscle, skin dermis, and pancreas were negative for MRC2.

CD276 was present in some types of normal tissues. It was found highly expressed (3+) in liver hepatocytes, and cardiac muscle. It had moderate expression (2+) in placenta villous cells, ovary stroma, germinal centers of the tonsils, Leydig cells of the testes, skin dermis, pancreas, and gastric, small intestine, and colonic glands and stroma. CD276 had mild (1+) expression in a small subset of renal tubules.

In vivo antitumor activities of BT1769 in osteosarcoma PDX models

BT1769 is a BTC that consists of a targeting *Bicycle* peptide that binds to MT1-MMP with high affinity ($K_D = 3.35$ nmol/L), which is linked to the cytotoxin MMAE *via* an enzymatically cleavable dipeptide linker (**Fig. 5A**; Supplementary Fig. S3; ref. 32). BT1769 has a short circulating plasma half-life *in vivo* (0.7 hour in mice) and a low molecular weight (3.9 kDa), the combination of which allows rapid accumulation of MMAE toxin in the tumor and fast elimination of non–tumor-bound BTC, thereby minimizing exposure of healthy tissue to the toxin (**Fig. 5B**). Moreover, this accumulation of BT1769-derived MMAE in the tumor gives rise to significant antitumor activity in an HT1080 xenograft model, which has high MT1-MMP expression (29), following 3.2 mg/kg weekly dosing.

BT1769 was generally well tolerated at a dose of 3 mg/kg once per week for 4 weeks. The average maximum weight loss across all models tested was 6.8%. BT1769 induced significantly prolonged EFS in all tested mice across all 6 osteosarcoma models. BT1769 showed objective responses (MCR) in 3 of 6 models. Two models (OS1, OS9) showed early progressive disease (PD1), and 1 model (OS31) showed later progressive disease (PD2; Supplementary Table S3; **Fig. 6A**). Although OS17 initially met the criteria for MCR after the treatment, recurrent tumor was observed 9 weeks after treatment. IHC staining of MT1-MMP showed the recurrent tumor had a low MT1-MMP expression level (H-score = 10) whereas the pretreatment tumor had relatively high MT1-MMP expression (H-score = 222; **Fig. 6D**). The models that experienced progressive disease had a median time to event for the treated versus control animals (EFS T/C) of 1.50 for OS9, 1.93 for OS1, and 3.02 for OS31 (Supplementary Table S3; **Fig. 6B**).
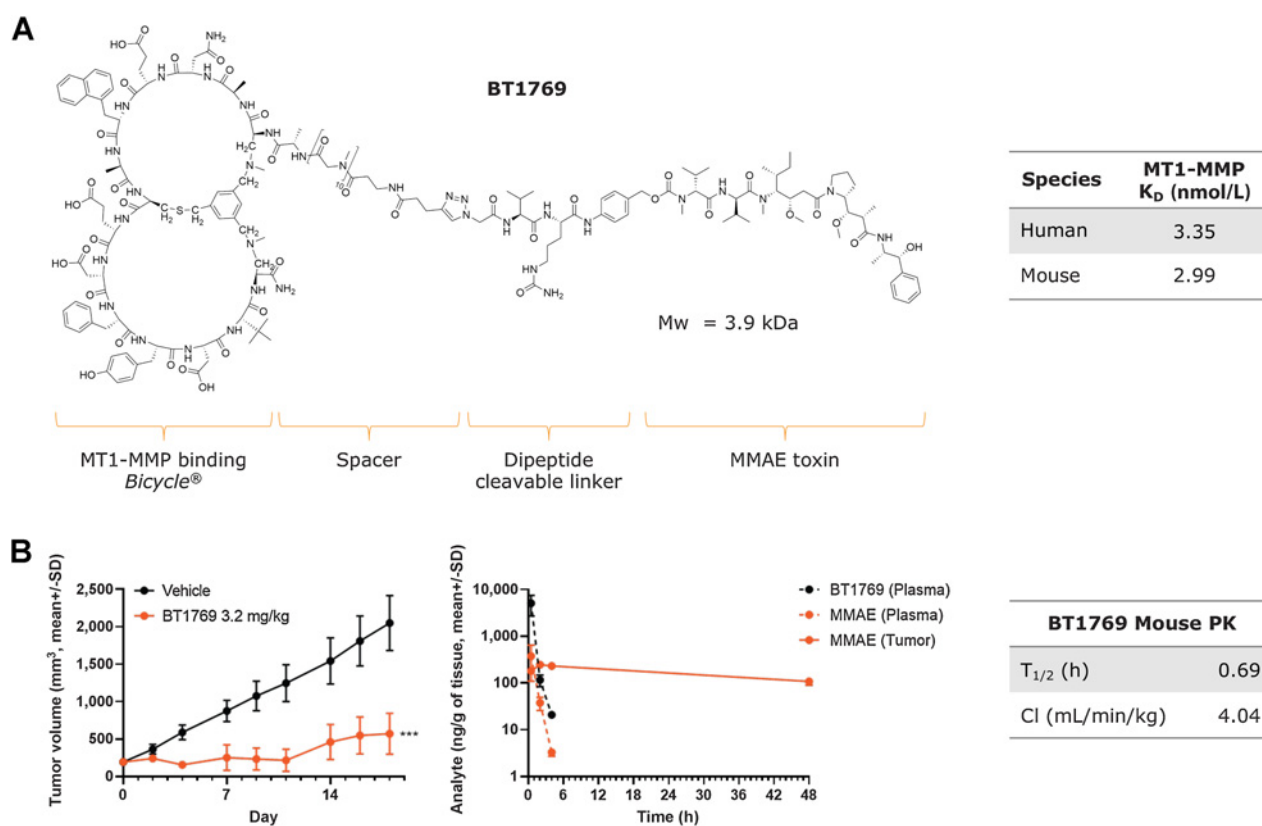
Figure 5.
Chemical structure, surface plasmon resonance, and pharmacokinetic analysis of BT1769. **A,** Chemical structure of BT1769, which exhibits high binding affinity to human and mouse MT1-MMP, as determined by SPR. **B,** Antitumor activity of 3.2 mg/kg BT1769 (IV, QW) in HT1080 xenograft-bearing mice is shown on the left ($P < 0.001$; two-way ANOVA). BT1769 concentration in plasma and MMAE concentrations in plasma and tumor are shown on the right. The table shows the half-life ($T_{1/2}$) and systemic clearance (Cl) of BT1769 in a naïve CD-1 mouse after IV dosing of 3 mg/kg BT1769.

RNA-seq data and IHC H-scores showed OS33 had the highest MT1-MMP expression level compared with OS1, OS17, OS2, OS9, and OS31 (**Fig. 6C**).

The MT1-MMP–negative Ewing sarcoma models (**Fig. 6E**) showed a PD1 with a median time to event for treated versus control animals (EFS T/C) of 1.15 for TC-71 and 1.25 for ES-1 (Supplementary Table S3; **Fig. 6A** and **B**). Details of statistical methods are provided in Statistical Methods Appendix and all testing results are provided in Supplementary Table S3. Supplementary Table S4 lists the passage number and growth characteristics of each of the tested xenografts.

Discussion

During the last several decades, much progress has been made in targeting cell-surface antigens. However, several immunotherapeutic agents failed to show sufficient efficacy in the clinical trials among patients with osteosarcoma (9, 13, 14). The major reason might be the paucity of tumor-specific antigens that are highly expressed in most osteosarcomas but not in normal tissues. Therefore, identifying high-confidence cell-surface antigens in osteosarcoma is necessary for the development of novel treatment strategies.

Most of the investigations of cell-surface immunotherapeutic targets have relied on transcriptomic data (33). Such an approach is based on the assumption that there is a direct correlation between RNA and protein expression level. However, such correlation might not be universal due to complex posttranscriptional and posttranslational mechanisms (34, 35). In the current study, we integrated the transcriptomic and proteomic data from osteosarcoma samples to identify high-confidence cell-surface proteins that are enriched at both RNA and protein levels. The results were further validated at the protein level with osteosarcoma cell lines, PDX models, and patient samples.

MT1-MMP has been reported to regulate cell-extracellular matrix degradation, cell invasion, and cancer metastasis (36). Rankin and colleagues (37) reported the high expression of MT1-MMP was associated with reduced overall survival in patients with osteosarcoma. Our previous work with a closely related analogue of the MT1-MMP targeting Bicycle peptide labelled with a radionuclide has demonstrated MT1-MMP specific accumulation of the peptide in the MT1-MMP expressing tumor tissue but not the normal tissues (29). Furthermore, the MT1-MMP–targeted BTC (BT1718), which contains a cleavable disulfide linker and maytansinoid payload, is currently being tested in a Phase I/IIa clinical trial in patients with advanced solid tumors. BT1718 has been well tolerated and showed encouraging activities (38), further supporting MT1-MMP as a therapeutic target.

Engelholm and colleagues (39) reported that MRC2 (uPARAP/endo180) is highly expressed in osteosarcoma samples. Blocking of MRC2 by a mAb led to a strong reduction of the tumor-induced bone destruction. Moreover, Nielsen and colleagues (27) reported an MRC2-targeted ADC that showed antitumor activity in MRC2-positive malignancies.
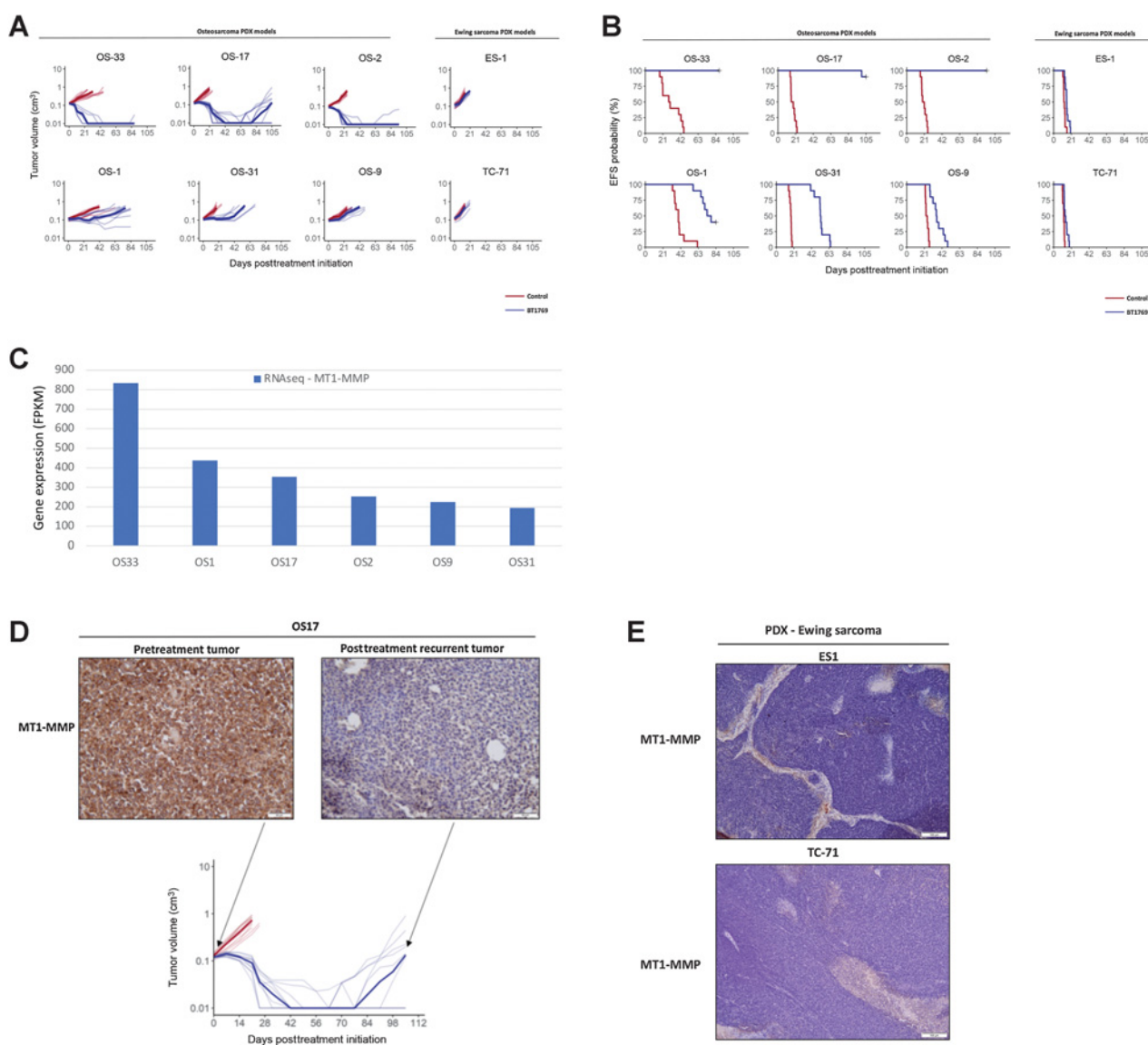
Figure 6.
Tumor volume and survival after BT1769 treatment in osteosarcoma preclinical models. **A,** BT1769 showed objective responses (MCR) in 3 osteosarcoma models, PD1 in 2 models (OS1, OS9), and PD2 in 1 model (OS31). The 2 Ewing sarcoma models (ES1, TC-71) had PD1. (MCR = maintained complete response. See appendix for detailed definitions.) Pale colored lines represent individual mice; dark colored lines show cohort median values. **B,** BT1769 induced significant improvement in EFS compared with control in all 6 of the osteosarcoma models tested (*P* < 0.05). **C,** RNA-seq data showed the expression level of MT1-MMP in the tested PDX models. **D,** MT1-MMP IHC staining of the OS17 recurrent tumor showed a low MT1-MMP expression level after initial MCR compared with the pretreatment tumor. **E,** MT1-MMP was negative in the Ewing sarcoma models (ES1, TC-71).

On the basis of our surfaceome profiling results, the efficacy and toxicity of the MRC2-targeted ADC is currently being evaluated in our preclinical osteosarcoma models.

CD276 (B7-H3) is a member of the B7 family of co-stimulatory molecules. It is reported to be highly expressed by tumor cells and tumor vasculatures in many cancers (40). Moreover, Wang and colleagues (41) demonstrated that CD276 was expressed in osteosarcoma and *in vitro* studies showed CD276 promoted osteosarcoma cell invasion (41). These studies provided evidence that CD276 is a promising pan-cancer antigen that warrants further development of immunotherapeutic modalities such as ADCs and CAR T cells (42).

Immunoconjugates and other compounds targeting cell-surface antigens have shown great potential in both hematologic and solid tumors (7). In recent years, our group has tested multiple ADCs in our osteosarcoma models such as glembatumumab vedotin, ABBV-085, and m276-PBD (14, 31, 43). Roth and colleagues (16) first reported that GPNMB was expressed in most osteosarcoma patient samples, and glembatumumab vedotin induced cytotoxic effects *in vitro* and *in vivo* (14). LRRC15 is expressed in multiple solid tumors, including osteosarcomas. In a PPTC preclinical study of the ADC ABBV-085 (conjugated to monomethyl auristatin E) in 7 PDX models, 6 had inhibited tumor growth, and 2 showed MCR (31). In a recent preclinical test, the CD276-targeted ADC M276-PBD showed a 92%

overall response rate in pediatric solid tumors, with 62% of models showing an MCR (43). This result further supported our surfaceome profiling results that CD276 is a promising immunotherapeutic target in osteosarcomas and in other pediatric solid tumors.

In the current study, an MT1-MMP–targeted BTC (BT1769) was tested in six osteosarcoma PDX models. BT1769 consists of a novel bicyclic targeting peptide that selectively binds MT1-MMP; a cytotoxin MMAE; and an enzymatically cleavable dipeptide linker. BT1769 showed potent antitumor activity against osteosarcoma PDX. The results validated our approach of the identification of the cell-surface targets, as well as the therapeutic potential of MT1-MMP–targeted therapies in osteosarcoma. However, in one of our models (OS17), although MCR was initially achieved, recurrent tumors developed, with a loss of MT1-MMP expression. As aforementioned, the expression levels of MMP14, MRC2, and CD276 did not affect survival and they are unlikely the major drivers in tumorigenesis of osteosarcoma. Thus, these targets may be prone to antigen escape as we observed in OS17. Also, all three targets have limited expression in some normal tissues. This may lead to on-target/off-tumor toxicities. Although preclinical testing showed promising results, the potential of these drugs in the treatment of osteosarcomas will need to be confirmed in future clinical trials.

We acknowledge the limitations of the current study. First, our proteo-transcriptomic profiling strategy excludes non-protein targets that could also be meaningful cell-surface targets. Also, mass spectrometry could be biased against less abundant proteins, and proteins that have a small number of tryptic peptides are hard to identify. The limited sensitivity of mass spectrometry may have led to missing some meaningful therapeutically accessible proteins (44). Also, different membrane protein extraction methods, may have different yields. The method used in the current study may also extract membrane proteins from other organelles such as the mitochondria. However, the localization of our candidate proteins was validated by flow cytometry and IHC. In the future, highly sensitive mass spectrometry and an optimized plasma membrane extraction method are needed to further investigate the surfaceome of osteosarcomas. Moreover, we acknowledge that small changes in the targeting moiety of the BTCs may lead to a different biodistribution profile. Therefore, it is important to further characterize BT1769 by assessing its *in vivo* distribution in tumor, blood, and healthy organs. Finally, all the PDX bearing mice were CB17SC scid−/− mice. Thus, further test of BT1769 in immunocompetent mouse models is needed to evaluate the role of the immune system in the remission process.

In conclusion, our integrated surfaceome profiling approach identified high-confidence osteosarcoma cell-surface targets that were validated at the protein level. The preclinical testing of the cell-surface antigen–targeting agents with cytotoxic payloads directed against these proteins shows promising responses providing further validation of proof of principle. These results suggest a pathway for developing cytotoxic agents targeting selected cell-surface antigens as treatment strategy for osteosarcomas.

Authors' Disclosures

Authors' Contributions

Y. Wang: Conceptualization, writing–original draft. **X. Tian:** Data curation, software, formal analysis, investigation, methodology, writing–original draft. **W. Zhang:** Investigation. **Z. Zhang:** Investigation. **R. Lazcano:** Investigation, writing–original draft. **P. Hingorani:** Writing–review and editing. **M.E. Roth:** Writing–review and editing. **J.D. Gill:** Writing–review and editing. **D.J. Harrison:** Writing–review and editing. **Z. Xu:** Investigation. **S. Jusu:** Investigation. **S. Kannan:** Investigation. **J. Wang:** Investigation. **A.J. Lazar:** Investigation. **E.J. Earley:** Resources. **S.W. Erickson:** Resources. **T. Gelb:** Resources, writing–original draft. **P. Huxley:** Resources. **J. Lahdenranta:** Resources. **G. Mudd:** Resources. **R.T. Kurmasheva:** Methodology. **P.J. Houghton:** Methodology. **M.A. Smith:** Funding acquisition, methodology, writing–review and editing. **E.A. Kolb:** Methodology. **R. Gorlick:** Conceptualization, supervision, funding acquisition, writing–review and editing.

Acknowledgments

References

1. Mirabello L, Troisi RJ, Savage SA. Osteosarcoma incidence and survival rates from 1973 to 2004: data from the surveillance, epidemiology, and end results program. Cancer 2009;115:1531–43.
2. Kager L, Zoubek A, Potschger U, Kastner U, Flege S, Kempf-Bielack B, et al. Primary metastatic osteosarcoma: presentation and outcome of patients treated on neoadjuvant Cooperative Osteosarcoma Study Group protocols. J Clin Oncol 2003;21:2011–8.
3. Sayles LC, Breese MR, Koehne AL, Leung SG, Lee AG, Liu HY, et al. Genome-informed targeted therapy for osteosarcoma. Cancer Discov 2019;9:46–63.
4. Davis KL, Fox E, Reid JM, Liu X, Minard CG, Weigel B, et al. ADVL1412: Initial results of a phase I/II study of nivolumab and ipilimumab in pediatric patients with relapsed/refractory solid tumors—a COG study. J Clin Oncol 2017;35(suppl 15):10526.
5. Coiffier B, Thieblemont C, Van Den Neste E, Lepeu G, Plantier I, Castaigne S, et al. Long-term outcome of patients in the LNH-98.5 trial, the first randomized study comparing rituximab-CHOP with standard CHOP chemotherapy in DLBCL patients: a study by the Groupe d'Etudes des Lymphomes de l'Adulte. Blood 2010;116:2040–5.
6. Kochenderfer JN, Somerville RPT, Lu T, Yang JC, Sherry RM, Feldman SA, et al. Long-duration complete remissions of diffuse large B-cell lymphoma after anti-CD19 chimeric antigen receptor T-cell therapy. Mol Ther 2017;25:2245–53.

7. Modi S, Saura C, Yamashita T, Park YH, Kim SB, Tamura K, et al. Trastuzumab deruxtecan in previously treated HER2-positive breast cancer. N Engl J Med 2020;382:610–21.

8. Ebb D, Meyers P, Grier H, Bernstein M, Gorlick R, Lipshultz SE, et al. Phase II trial of trastuzumab in combination with cytotoxic chemotherapy for treatment of metastatic osteosarcoma with human epidermal growth factor receptor 2 overexpression: a report from the Children's Oncology Group. J Clin Oncol 2012;30:2545–51.

9. Weigel B, Malempati S, Reid JM, Voss SD, Cho SY, Chen HX, et al. Phase II trial of cixutumumab in children, adolescents, and young adults with refractory solid tumors: a report from the Children's Oncology Group. Pediatr Blood Cancer 2014;61:452–6.

10. Demetri GD, Luke JJ, Hollebecque A, Powderly JD, Spira AI, Subbiah V, et al. First-in-human phase I study of ABBV-085, an antibody-drug conjugate (ADC) targeting LRRC15, in sarcomas and other advanced solid tumors. J Clin Oncol 2019;37:3004.

11. Kopp LM, Malempati S, Krailo M, Gao Y, Buxton A, Weigel BJ, et al. Phase II trial of the glycoprotein nonmetastatic B-targeted antibody-drug conjugate, glembatumumab vedotin (CDX-011), in recurrent osteosarcoma AOST1521: a report from the Children's Oncology Group. Eur J Cancer 2019;121:177–83.

12. Hingorani P, Krailo MD, Buxton A, Hutson PR, Davis J, Janeway KA, et al. Phase II study of antidisialoganglioside antibody, dinutuximab, in combination with GM-CSF in patients with recurrent osteosarcoma (AOST1421): a report from the Children's Oncology Group. J Clin Oncol 2020;38(suppl 15):10508.

13. Cao Y, Roth M, Piperdi S, Montoya K, Sowers R, Rao P, et al. Insulin-like growth factor 1 receptor and response to anti-IGF1R antibody therapy in osteosarcoma. PLoS One 2014;9:e106249.

14. Roth M, Barris DM, Piperdi S, Kuo V, Everts S, Geller D, et al. Targeting glycoprotein NMB with antibody-drug conjugate, glembatumumab vedotin, for the treatment of osteosarcoma. Pediatr Blood Cancer 2016;63:32–8.

15. Roth M, Linkowski M, Tarim J, Piperdi S, Sowers R, Geller D, et al. Ganglioside GD2 as a therapeutic target for antibody-mediated therapy in patients with osteosarcoma. Cancer 2014;120:548–54.

16. Hingorani P, Zhang W, Kurmasheva R, Zhang Z, Wang Y, Xu Z, et al. Abstract LB-217: preclinical evaluation of trastuzumab deruxtecan (T-DXd; DS-8201a), a HER2 antibody-drug conjugate, in pediatric solid tumors by the Pediatric Preclinical Testing Consortium (PPTC). Cancer Res 2020;80:LB–217.

17. Mudd GE, Brown A, Chen L, van Rietschoten K, Watcham S, Teufel DP, et al. Identification and optimization of EphA2-selective bicycles for the delivery of cytotoxic payloads. J Med Chem 2020;63:4107–16.

18. Bennett G, Brown A, Mudd G, Huxley P, Van Rietschoten K, Pavan S, et al. MMAE delivery using the bicycle toxin conjugate BT5528. Mol Cancer Ther 2020;19:1385–94.

19. Houghton PJ, Morton CL, Tucker C, Payne D, Favours E, Cole C, et al. The pediatric preclinical testing program: description of models and early testing results. Pediatr Blood Cancer 2007;49:928–40.

20. Rokita JL, Rathi KS, Cardenas MF, Upton KA, Jayaseelan J, Cross KL, et al. Genomic profiling of childhood tumor patient-derived xenograft models to enable rational clinical trial design. Cell Rep 2019;29:1675–89.e9.

21. Sowers R, Wenzel BD, Richardson C, Meyers PA, Healey JH, Levy AS, et al. Impairment of methotrexate transport is common in osteosarcoma tumor samples. Sarcoma 2011;2011:834170.

22. Zybailov BL, Florens L, Washburn MP. Quantitative shotgun proteomics using a protease with broad specificity and normalized spectral abundance factors. Mol Biosyst 2007;3:354–60.

23. Binder JX, Pletscher-Frankild S, Tsafou K, Stolte C, O'Donoghue SI, Schneider R, et al. COMPARTMENTS: unification and visualization of protein subcellular localization evidence. Database (Oxford) 2014;2014:bau012.

24. Lomize AL, Hage JM, Pogozheva ID. Membranome 2.0: database for proteome-wide profiling of bitopic proteins and their dimers. Bioinformatics 2018;34:1061–2.

25. Rathore R, Caldwell KE, Schutt C, Brashears CB, Prudner BC, Ehrhardt WR, et al. Metabolic compensation activates pro-survival mTORC1 signaling upon 3-phosphoglycerate dehydrogenase inhibition in osteosarcoma. Cell Rep 2021;34:108678.

26. Wu CC, Beird HC, Andrew Livingston J, Advani S, Mitra A, Cao S, et al. Immuno-genomic landscape of osteosarcoma. Nat Commun 2020;11:1008.

27. Nielsen CF, van Putten SM, Lund IK, Melander MC, Norregaard KS, Jurgensen HJ, et al. The collagen receptor uPARAP/Endo180 as a novel target for antibody-drug conjugate mediated treatment of mesenchymal and leukemic cancers. Oncotarget 2017;8:44605–24.

28. Teufel DM, Mudd G, Pavan S. Peptide ligands for binding to MT1-MMP2018. Available from: https://patentscope.wipo.int/search/en/detail.jsf?docId=WO2018115204.

29. Eder M, Pavan S, Bauder-Wust U, van Rietschoten K, Baranski AC, Harrison H, et al. Bicyclic peptides as a new modality for imaging and targeting of proteins overexpressed by tumors. Cancer Res 2019;79:841–52.

30. Samaras P, Schmidt T, Frejno M, Gessulat S, Reinecke M, Jarzab A, et al. ProteomicsDB: a multi-omics and multi-organism resource for life science research. Nucleic Acids Res 2020;48:D1153-D63.

31. Hingorani P, Roth ME, Wang Y, Zhang W, Gill JD, Harrison DJ, et al. ABBV-085, antibody-drug conjugate targeting LRRC15, is effective in osteosarcoma: a report by the Pediatric Preclinical Testing Consortium. Mol Cancer Ther 2021;20:535–40.

32. Teufel DM, Mudd G, Pavan S. Peptide derivatives having novel linkage structures. World patent WO2018115203A1. Available from: https://patentscope.wipo.int/search/en/detail.jsf?docId=WO2018115203.

33. Bosse KR, Raman P, Zhu Z, Lane M, Martinez D, Heitzeneder S, et al. Identification of GPC2 as an oncoprotein and candidate immunotherapeutic target in high-risk neuroblastoma. Cancer Cell 2017;32:295–309.e12.

34. Gunawardana Y, Niranjan M. Bridging the gap between transcriptome and proteome measurements identifies posttranslationally regulated genes. Bioinformatics 2013;29:3060–6.

35. Perna F, Berman SH, Soni RK, Mansilla-Soto J, Eyquem J, Hamieh M, et al. Integrating proteomics and transcriptomics for systematic combinatorial chimeric antigen receptor therapy of AML. Cancer Cell 2017;32:506–19.e5.

36. Uchibori M, Nishida Y, Nagasaka T, Yamada Y, Nakanishi K, Ishiguro N. Increased expression of membrane-type matrix metalloproteinase-1 is correlated with poor prognosis in patients with osteosarcoma. Int J Oncol 2006;28:33–42.

37. Biswas S, Rankin K, Long A, Nisar S, Gerrand C, Dildey P, et al. Abstract 5580: membrane-type 1 matrix metalloproteinase (MT1-MMP): a predictive biomarker of chemotherapy response in osteosarcoma. In: Proceedings of the 103rd Annual Meeting of the American Association for Cancer Research; 2012 Mar 31-Apr 4; Chicago, IL. Philadelphia (PA): AACR; Cancer Res 2012;72(8 Suppl): Abstract nr 5580. doi:1538-7445.AM2012-5580.

38. Cook NBU, Evans TRJ, Biondo A, Germetaki T, Randhawa M, Godfrey L, et al., editors. Pharmacokinetic (PK) assessment of BT1718: A phase I/IIa study of BT1718, a first in class bicycle toxin conjugate (BTC), in patients (pts) with advanced solid tumors [abstract]. Ann Oncol 2019;30:v159–93.

39. Engelholm LH, Melander MC, Hald A, Persson M, Madsen DH, Jurgensen HJ, et al. Targeting a novel bone degradation pathway in primary bone cancer by inactivation of the collagen receptor uPARAP/Endo180. J Pathol 2016;238:120–33.

40. Seaman S, Zhu Z, Saha S, Zhang XM, Yang MY, Hilton MB, et al. Eradication of tumors through simultaneous ablation of CD276/B7-H3–positive tumor cells and tumor vasculature. Cancer Cell 2017;31:501–15.e8.

41. Wang L, Zhang Q, Chen W, Shan B, Ding Y, Zhang G, et al. B7-H3 is overexpressed in patients suffering osteosarcoma and associated with tumor aggressiveness and metastasis. PLoS One 2013;8:e70689.

42. Majzner RG, Theruvath JL, Nellan A, Heitzeneder S, Cui Y, Mount CW, et al. CAR T cells targeting B7-H3, a pan-cancer antigen, demonstrate potent preclinical activity against pediatric solid tumors and brain tumors. Clin Cancer Res 2019;25:2560–74.

43. Kendersky NM, Lindsay J, Kolb EA, Smith MA, Teicher BA, Erickson SW, et al. The B7-H3–targeting antibody-drug conjugate m276-SL-PBD is potently effective against pediatric cancer preclinical solid tumor models. Clin Cancer Res 2021;27:2938–46.

44. Zhao W, Fitzgibbon M, Bergan L, Clegg N, Crispin D, Mills GB, et al. Identifying abundant immunotherapy and other targets in solid tumors: integrating RNA-seq and mass spectrometry proteomics data sets. Cancer J 2017;23:108–14.